First publ. in: Fungal Genetics and Biology 35 (2002), pp. 99-113

Four or More Species of *Cladosporium* Sympatrically Colonize *Phragmites australis*

Stefan G. R. Wirsel,* Christiane Runge-Froböse,* Dag G. Ahrén,† Eric Kemen,* Richard P. Oliver,‡ and Kurt W. Mendgen*,[1]

**Lehrstuhl für Phytopathologie, Fachbereich Biologie, Universität Konstanz, Universitätstr. 10, 78457 Konstanz, Germany; †Microbial Ecology, Ecology Building, Lund University, 22362 Lund, Sweden; and ‡Australian Centre for Necrotrophic Fungal Pathogens, School of Biological Sciences, Murdoch University, Perth, Western Australia 6150, Australia*

Accepted for publication November 8, 2001; published online January 24, 2002

Wirsel, S. G. R., Runge-Froböse, C., Ahrén, D. G., Kemen, E., Oliver, R. P., and Mendgen, K. W. 2002. Four or more species of *Cladosporium* sympatrically colonize *Phragmites australis. Fungal Genetics and Biology* 35, 99–113. A collection of *Cladosporium* has been recovered from common reed growing at Lake Constance (Germany). High-resolution cryo-scanning electron microscopy revealed that *Cladosporium* isolates from reed are diverse. Morphologically, we distinguished three species, viz. *C. herbarum, C. oxysporum,* and *Cladosporium* sp. Internal transcribed spacer (ITS) sequence analysis supported these results and, moreover, separated the most common species, *C. oxysporum,* into two subclades. Two additional phylogenies were generated to gain support for this finding. The first, differentiating fungi by their capacities to metabolize different carbon sources, showed correlation with morphology. The second, based on actin gene sequences, showed the same overall topology as that of the ITS tree, but resulted in a higher resolution indicating the existence of four or more species of *Cladosporium* on reed. A nested PCR assay targeting variable sequences within actin introns indicated that these four species sympatrically colonize reed. There was no evidence for mutual exclusion on or within the host or specialization for host habitats or organs.

[1] To whom correspondence should be addressed. Fax: (+49) 7531 883035. E-mail: kurt.w.mendgen@uni-konstanz.de.

Index Descriptors: Cladosporium; Septoria; Mycosphaerella; reed; *Phragmites australis;* Actin; ITS; BIOLOG.

As part of a long-term program designed to integrate several aspects of freshwater ecology at Lake Constance (Germany), we have investigated the interaction of fungi with common reed (*Phragmites australis* (Cav.) Trin. ex Steudel, Poaceae) and their influence on the productivity and health of the host. Reed is a wetland plant that can form homogenous belts around freshwater lakes. In an earlier report, we described a collection of reed-associated fungi obtained during a study designed to identify specialization toward the host organ and/or the position of the host within the reed belt (Wirsel *et al.,* 2001). These isolates were recovered from surface-sterilized root, stem, and leaf samples and were classified by morphological traits at the genus level. For each group, we determined the internal transcribed spacer (ITS) sequence of one or two isolates which confirmed the morphological grouping in most cases.

Here, we analyze in detail the taxonomy, physiology, and ecology of one of the most common genera from that collection, *Cladosporium*, which represented about 15% of all isolates. The anamorph genus *Cladosporium* is one of the most widespread and prevalent of all fungal genera (David, 1997). It lacks morphological structures that would firmly place species in an evolutionary context. Molecular data are therefore important to reveal phyloge-

netic relationships within this genus. In an earlier study (Curtis *et al.*, 1994) partial rDNA sequences of several independent isolates of *C. fulvum* (syns. *Fulvia fulva, Mycovellosiella fulva*) and single isolates of *C. herbarum, C. oxysporum, C. cladosporioides,* and *C. sphaerospermum* indicated that these species together might form a monophyletic clade. Where it is known, species of *Cladosporium* have *Mycosphaerella* (Mycosphaerellaceae, Dothideales) teleomorphs. *Mycosphaerella* is also a large genus containing many important plant pathogens, such as *M. graminicola* (anamorph: *Septoria tritici*), which is a serious wheat pathogen.

The present study addresses three questions about the ecology of reed-associated Cladosporia. First, do all isolates studied belong to one or more species? This problem was approached by a scanning electron microscopy (SEM)-enhanced morphological characterization and by building a molecular phylogeny based on the ITS region and the actin gene. Second, is there a specialization for host habitat and/or organ? This hypothesis was investigated by correlating carbon utilization patterns obtained from BIOLOG microtiter plates with sampling data and by comparing the most parsimonious actin/ITS tree with several constrained trees that grouped strains according to sampling details. Third, is there evidence for mutual exclusion of the four different clades of Cladosporia on reed? For this purpose we developed a nested PCR assay based on divergent actin gene sequences that differentially detects different taxa in environmental DNA.

MATERIALS AND METHODS

Plant and Fungal Materials

The fungal isolates used in this study (Table 1) originate from a sampling program at two locations 6.8 km apart at opposite shores of the Bodman peninsula at Lake Constance (Germany) (Wirsel *et al.*, 2001). At each location, two reed habitat types, separated by about 50 m, were sampled. One type was at the lakeward side of the reed belt and was permanently flooded under normal water levels ("flooded site"). The other was at the landward side of the reed belt and only flooded during extreme high-water periods ("dry site"). Reference cultures are listed in Table 2. Fungi were grown on 2% malt agar (Biomalt; Villa Natura Gesundprodukte GmbH, Kirn, Germany) at 22°C under long-wave UV light. Representative isolates described in this work were deposited at CBS (Utrecht, Netherlands).

Clumps of three to five culms—including their root systems—that covered a surface area of about 30 × 30 cm were dug out in August 1998, August 1999, and April 2000 at the same four sites at Lake Constance described above. The April harvests represented young shoots of about 20 cm height, whereas the August samples represented the peak biomass. We divided the August plants into root, stem, and leaf samples, whereas the April plants were divided into root and shoot samples, the latter comprising stems and unfolded leaves. All samples were thoroughly washed under running tap water and stored at −70°C until DNA isolation.

Low-Temperature Scanning Electron Microscopy (LTSEM)

Fungal samples were taken from malt agar cultures (approx. 4 mm^2), mounted on aluminum stubs with Tissue-tek (Sakura, Tokyo, Japan) and frozen by plunging holder and sample into nitrogen slush. Samples were then inserted into the Alto 2500 (Gatan, Oxford, U.K.) preparation chamber by means of the vacuum transfer device and mounted onto the cryostage cooled to −130°C. Once the preparation chamber was at high vacuum (pressure $<4 \times 10^{-4}$ Pa), the cryostage temperature was raised to −90°C for 30 s and then cooled again to −130°C. Subsequently, samples were sputter-coated with a 6-nm-thick platinum layer and immediately transferred to the SEM cryostage. Samples were examined at −125°C with a Model S-4700 field emission scanning electron microscope (Hitachi, Tokyo, Japan) running either in the high-resolution mode, the normal mode, or the analytical mode, depending on the magnification used. SEM micrographs were recorded digitally at an acceleration voltage of 2–5 kV.

Registration of Substrate Utilization Patterns in BIOLOG Microplates

We used BIOLOG SF-N plates (Merlin Diagnostika GmbH, Bornheim, Germany) that contained 95 different carbon sources in a microtiter plate format to determine the range of catabolic capabilities of the fungi tested. Inoculum was obtained by suspending conidia with a sterile spatula from fresh agar cultures in 5 ml 0.2% carrageenan type II (Sigma, Deisenhofen, Germany); 100 μl of a conidial suspension adjusted to an OD_{590} of 0.011 was used to inoculate each well. Incubation was at 21°C in the dark. Since the isolates exhibited differential growth rates on malt agar plates (data not shown) we decided not to

TABLE 1
Characterization of *Cladosporium* Isolates Recovered from Reeds at Lake Constance

Strain	Location[1]	Habitat[2]	Organ[3]	Morphology	ITS type[4]	Actin accession	BIOLOG
4/97-48	M	f	l	*C. herbarum*	C	AJ300320	See Table 4
6/97-44	M	f	1	*C. herbarum*	C	As CBS 812.71*	n.d.
315W	M	d	r	*C. herbarum*	C	AJ300323	See Table 4
6/97-32	R	d	r	*C. herbarum*	C	As 5/97-9	See Table 4
4/97-5	M	f	r	*C. herbarum*	C	n.d.	n.d.
5/97-20	M	f	r	*C. herbarum*	C	n.d.	n.d.
5/97-9	M	f	r	*C. herbarum*	C	AJ300315	See Table 4
6/97-3	M	f	r	*C. herbarum*	C	n.d.	n.d.
4/97-19	M	f	r	*C. herbarum*	n.d.	n.d.	n.d.
4/97-101	R	f	r	*C. herbarum*	C	n.d.	n.d.
4/97-41	R	f	r	*C. herbarum*	C	n.d.	n.d.
4/97-49	R	f	r	*C. herbarum*	C	n.d.	n.d.
6/97-12	R	f	r	*C. herbarum*	n.d.	n.d.	n.d.
4/97-6	M	f	s	*C. herbarum*	C	As 315W	See Table 4
4/97-12	M	f	s	*C. herbarum*	n.d.	n.d.	n.d.
6/97-4	R	f	s	*C. herbarum*	C	As CBS 812.71*	See Table 4
6/97-56	R	f	s	*C. herbarum*	n.d.	n.d.	n.d.
6/97-48	M	f	l	*C. oxysporum*	A	n.d.	n.d.
6/97-49	M	f	l	*C. oxysporum*	A	n.d.	n.d.
4/97-17	R	f	l	*C. oxysporum*	A	AJ300322	See Table 4
6/97-47	R	f	l	*C. oxysporum*	A	n.d.	n.d.
6/97-46	M	f	l	*C. oxysporum*	n.d.	n.d.	n.d.
6/97-68	M	d	r	*C. oxysporum*	A	AJ300313	See Table 4
5/97-22	M	d	r	*C. oxysporum*	A	n.d.	n.d.
5/97-83	M	d	r	*C. oxysporum*	A	AJ300316	n.d.
A14	R	d	r	*C. oxysporum*	A	As 4/97-17	See Table 4
RD294	R	d	r	*C. oxysporum*	A	AJ300311	See Table 4
5/97-10	R	d	r	*C. oxysporum*	n.d.	n.d.	n.d.
4/97-11	R	f	r	*C. oxysporum*	A	n.d.	n.d.
4/97-3	R	f	r	*C. oxysporum*	A	n.d.	n.d.
6/97-2	R	f	r	*C. oxysporum*	A	As CBS 401.80*	See Table 4
6/97-5	R	f	r	*C. oxysporum*	A	As 4/97-17	See Table 4
4/97-21	R	f	r	*C. oxysporum*	A	As 6/97-68	n.d.
4/97-42	R	f	r	*C. oxysporum*	n.d.	n.d.	n.d.
5/97-21	M	f	r	*C. oxysporum*	B	n.d.	n.d.
5/97-17	M	d	s	*C. oxysporum*	A	As 4/97-17	See Table 4
6/97-34	M	d	s	*C. oxysporum*	B	AJ300314	n.d.
5/97-111	R	f	s	*C. oxysporum*	A	AJ300318	See Table 4
4/97-20	M	f	s	*C. oxysporum*	B	AJ300321	n.d.
5/97-8	M	f	s	*C. oxysporum*	B	AJ300317	n.d.
4/97-2	R	f	s	*C. oxysporum*	B	As 6/97-34	See Table 4
5/97-11	R	f	s	*C. oxysporum*	B	AJ300319	See Table 4
A13	R	f	r	*C.* sp.	D	AJ300312	See Table 4
4/97-4	R	f	r	*C.* sp.	D	As A13	See Table 4

Note. Strains were sorted first by morphology and then by organ and site of isolation, respectively.
* See Table 2.
[1–3] Denotes the origin of the strains: [1]R/M, location: Reichenau/Mainau; [2]f/d, position in reed belt: flooded/dry; [3]r/s/l, host organ: root/stem/leaf.
[4] ITS types A–D received EMBL Accession Nos. AJ300332, AJ300337, AJ300333, and AJ300336, respectively. n.d., not determined.

score the results after a fixed incubation period, but at several time points as described before (Dobranic and Zak, 1999). For scoring, we recorded absorbances every other day by scanning plates on a Mikrotek Scanmaker 3 with the Adobe Photoshop 4.0 software. Files were saved in TIFF format and imported into the Multi Analyst 1.0.2 software (Bio-Rad GmbH, München, Germany) to record average pixel densities. Results were transformed into a Microsoft Excel 98 datasheet to subtract water controls and to adjust negative values to zero. For each time point

TABLE 2
Reference Cultures Used for Characterization of *Cladosporium* Isolates from Reed

Reference strain	Host plant	Location	ITS accession	Actin accession
C. oxysporum CBS 125.80*	*Cirsium vulgare*	Netherlands	AJ300332	AJ300325
C. cladosporioides CBS 169.54*	*Arundo* sp.	Kew, England	AJ300335	AJ300329
C. cladosporioides CBS 401.80*	*Triticum aestivum*	Netherlands	AJ300334	AJ300328
C. tenuissimum CBS 674.82*	*Gossypium* sp.	Jaffa, Israel	AJ300331	AJ300324
C. herbarum CBS 812.71*	*Polygonatum odoratum*	Lisen, Czechoslovakia	AJ300333	AJ300326
C. fulvum Dutch Race 4†	*Lycopersicon esculentum*	Netherlands	L25430	AJ300327
Septoria tritici L951#	*Triticum aestivum*	England	AJ300330	AJ300310

* Isolation details as on CBS listings.
† Curtis *et al.* (1994).
# Received from D. B. Collinge (Department of Plant Biology, KVL, Frederiksberg, Denmark).

we formed the sum of the 95 corrected pixel densities to create kinetics. For the following calculations, we used the data sets corresponding to the beginning of the respective plateaus. We defined four classes for growth, i.e., 0–1–2–3, to better differentiate between any two strains growing either vigorously or poorly on a particular carbon source. In such a case a 0–1 matrix would record both results as "1" but the extended matrix would note a "1" versus a "3." We defined the four classes from 0–15, 15–30, 30–60, and 60–100%, respectively; 100% indicates maximum density obtained with any carbon source (mostly glucose) on a given microtiter plate. The resulting data set was exported to the software package PAUP 4.0d64 (Swofford, 2000). Maximum-parsimony analysis used a matrix that weighted the growth differences according to the four classes explained above and the Wagner method implemented in PAUP 4.0d64 with equal weighting. Using stepwise addition of sequences, heuristic searches with 1000 bootstrap replicates were performed using tree bisection–reconnection (TBR). Branches with more than 50% support were used further in unrooted phylograms.

DNA Extraction, PCR, and Sequence Reactions

For the preparation of fungal genomic DNA, mycelial material was removed from agar plates with a sterile scalpel, transferred to an Eppendorf tube, and flash-frozen in liquid nitrogen. During thawing, micropestles (Biozym Diagnostik GmbH, Hessisch Oldendorf, Germany) were used to improve lysis. After adding 500 μl of a 10% suspension of Chelex 100 cation exchange resin (Bio-Rad GmbH) in sterile water and mixing for 5 s, incubation for 1 h at 65°C followed. The suspension was then mixed for 5 s and incubated for 5 min at 95°C. The supernatant resulting from a centrifugation for 5 min at 14,000 rpm was transferred to a fresh tube and kept at −20°C.

Plant genomic DNA was isolated from tissue samples stored at −70°C. Several cleaned parts of the same organ from one individual plant were pooled and homogenized with mortar and pestle in the presence of liquid nitrogen, resulting in about 5 ml of powdered material. About 100 mg powder was processed with the NucleoSpin Plant genomic DNA kit (Macherey-Nagel GmbH, Düren, Germany) following the instructions provided. DNA quality was controlled by agarose gel electrophoresis.

PCRs were carried out in a MJ Research PTC100 thermocycler (Biozym Diagnostik GmbH) to generate template DNA for sequencing. Fungal ITS regions were amplified with ITS1F as forward and ITS4 as reverse primer (White *et al.*, 1990; Gardes and Bruns, 1993). Reaction mixtures contained 0.5 μl fungal DNA solution in 50 μl of reaction mix (1× PCR buffer (MBI Fermentas GmbH, St. Leon-Roth, Germany), 1.5 mM $MgCl_2$, 0.2 mM dNTPs, 0.5 mg/ml bovine serum albumin, 0.3 μM each primer, and 0.04 U/μl of recombinant *Taq* Polymerase (MBI Fermentas)). An initial denaturation step of 94°C for 150 s was followed by 15 cycles of a touch-down PCR protocol: 94°C for 30 s, 70°C for 30 s with a decrease of 1°C per cycle, and 72°C for 30 s. This was immediately succeeded by 30 cycles of the following protocol: 94°C for 30 s, 55°C for 30 s, and 72°C for 30 s plus one additional second per cycle. After a final extension at 72°C for 10 min, reactions were cooled to 2°C. Fungal actin gene fragments were amplified using primers FungAct.F1 and FungAct.R1 (Table 3) that were designed during this study based on fungal reference sequences currently available in public sequence databases. PCR conditions were as for ITS fragments with the exception that the primer concentration was set at 1 μM and the final annealing temperature was

TABLE 3
Primers Designed during This Study

Primer	Orientation	Target sequence	Target organisms	Sequence (5′ to 3′)
Pa-ITS.F1	Forward	ITS1	*P. australis*	CGGGAGGGGAGGGGACGAAACAGAA
Pa-ITS.R1	Reverse	ITS2	*P. australis*	GGTACGCCGGCAGCCCCAACTTC
FungAct.F1	Forward	Actin	Fungi	TGGCAYCAYACITTYTAYAAYGA
FungAct.R1	Reverse	Actin	Fungi	CCICCIATCCAIACIGARTAYTT
CladAct.F1	Forward	Actin	*Cladosporium* spp.	CGTYCGYGACATCAAGGAG
CladAct.R1	Reverse	Actin	*Cladosporium* spp.	CTGGCTSGCGGTYTGGAT
CladAct.F3	Forward	Actin	*Cladosporium* spp.	GCCGTGACTTGACCGACTAC
CladAct.R3	Reverse	Actin	*Cladosporium* spp.	CCGGGGTACATGGTGGTAC
A14Act.R1	Reverse	Actin	*C. oxysporum* (A14)	TGCAGAAATGAGAAGGAAGTGAAC
4/97-2Act.R1	Reverse	Actin	*C. oxysporum* (4/97-2)	GACTGTGCGGTTTGTTAGCATCTT
315WAct.R1	Reverse	Actin	*C. herbarum* (315W)	GTGTGGGATTTCAAAGTCGGA
A13Act.R1	Reverse	Actin	*C* sp. (A13)	AGACTGTGTCATGTTAGCAACTTGAG

50°C after 15 cycles of the touch-down block. PCR fragments were purified with the QIAquick PCR Purification Kit (Qiagen GmbH, Hilden, Germany).

We designed PCR primers (Pa-ITS.F1 and Pa-ITS.R1; see Table 3) directed against the published ITS sequence of *P. australis* (Accession No. AF019810) to control for general amplificability of plant DNA preparations. Assays contained 0.5 μl of plant DNA in a volume of 19.5 μl of reaction mix (same as above). Cycle conditions were as for fungal ITS fragments (see above) with the exception that the final annealing temperature was set at 58°C after 10 cycles of a touch-down block.

PCR fragments were subjected to sequencing reactions using the ABI Prism BigDye Terminator Cycle Sequencing Kit (PE Applied Biosystems, Weiterstadt, Germany) according to the provided instructions. For ITS fragments primers were ITS1F, ITS2, ITS3, and ITS4 (White *et al.*, 1990; Gardes and Bruns, 1993). For actin gene fragments primers were FungAct.F1, FungAct.R1, CladAct.F1, and CladAct.R1 (Table 3). The latter two were designed during this study to match actin sequences from all isolates of the genus *Cladosporium*. DNA sequences were determined on an ABI377 automated sequencing system (PE Applied Biosystems). DNA sequences were assembled using the program SeqMan from the DNASTAR software package (GATC GmbH, Konstanz, Germany).

Sequences obtained during this work have been submitted to the EMBL database and have been assigned the Accession Nos. AJ300310 to AJ300337.

Phylogenetic Analysis

Pairwise alignments of sequences were carried out with the Martinez/Needleman-Wunsch algorithm implemented in the DNASTAR module MegAlign. Multiple alignments were created with the Clustal algorithm, which is implemented in the same module, and were manually improved and exported to the software package PAUP 4.0d64 (Swofford, 2000). The taxa were added by stepwise addition and analyzed using maximum-parsimony with equal weighting of the nucleotides. Gaps were treated as missing characters. The confidence of phylogenetic trees was estimated with 1000 heuristic bootstrap replicates using the tree bisection–reconnection (TBR) branch-swapping algorithm. Bootstrap values below 50% were collapsed. ITS and actin datasets were rooted using *S. tritici* as outgroup. Alignments of ITS and actin trees were deposited at the TreeBase database (http://www.herbaria.harvard.edu/treebase/).

Concordance of the ITS and actin datasets was analyzed with the partition homogeneity test included in PAUP 4.0d64 by using 1000 repartitions with MAXTREES set to 1000.

To compare alternative topologies the Kishino–Hasegawa likelihood test implemented in PAUP 4.0.d64 was used. Standard deviation from the original most parsimonious tree and P*, where P* shows whether a tree is significantly worse than the most parsimonious tree, were used to test whether hypothetical topologies could be rejected with confidence.

Nested PCR Assay

We developed a nested PCR assay based on the actin gene sequences established during this work to detect and differentiate distinct types of *Cladosporium* in reed DNA. The first amplification step relied on primers CladAct.F3 and CladAct.R3 (Table 3) that were designed to match actin sequences from all Cladosporia. PCR conditions

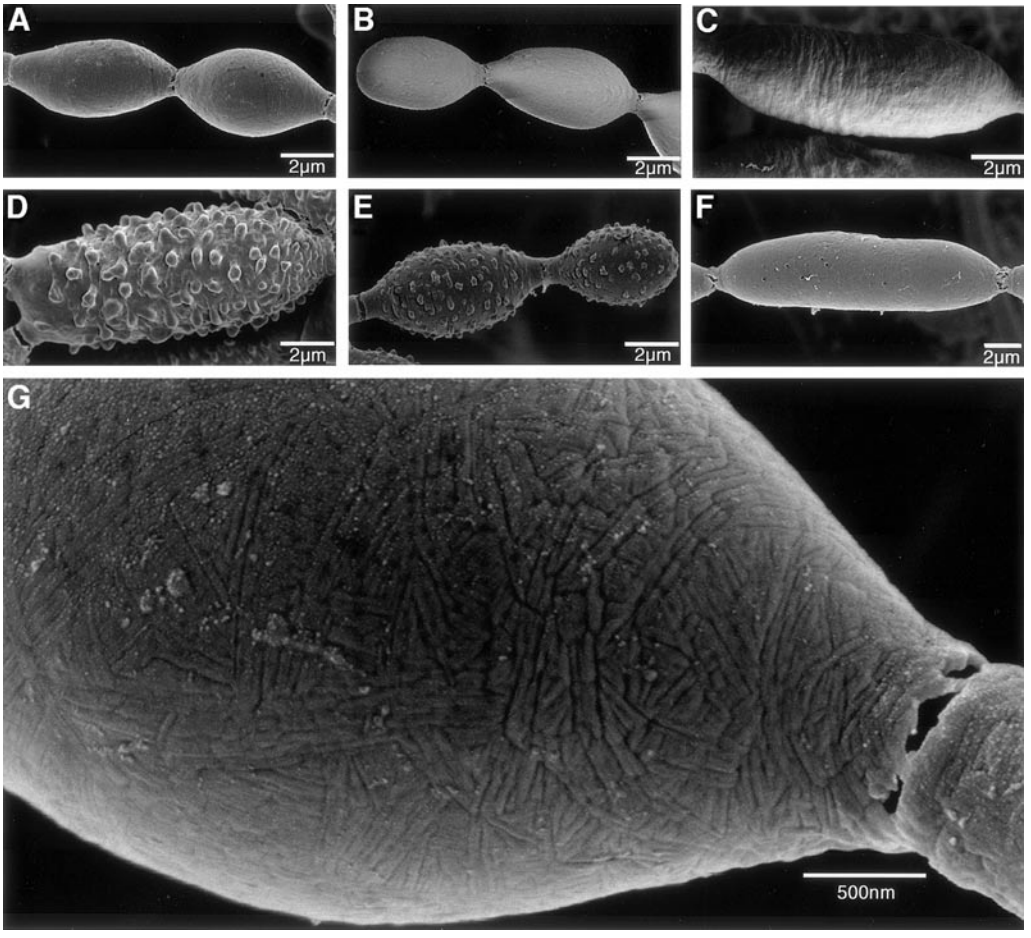

FIG. 1. LTSEM of native conidia from reference cultures. (A) *Cladosporium oxysporum* CBS 125.80; (B) *C. tenuissimum* CBS 674.82; (C) *C. cladosporioides* CBS 401.80; (D) *C. herbarum* CBS 812.71; (E) *C. cladosporioides* CBS 169.54; (F) *C. fulvum* Dutch Race 4; (G) *C. oxysporum* CBS 125.80 (higher magnification than that of A). For details of isolates, see Table 2.

were generally as above except that the annealing temperature was set to 62°C after 10 cycles of a touch-down block with a decrease of 1°C per cycle. The second PCR made use of variable intron sequences discovered in *Cladosporium* actin genes to differentiate between products from the first step. In all cases, the forward primer was CladAct.F1, which matched all Cladosporia, whereas four different reverse primers were placed within the introns to match only the particular strains from which it was derived (Table 3). Reaction mixtures were generally as described above with the exception that 1 µl of a 10-fold dilution of the first PCR step was used as template in a total volume of 20 µl. Cycling parameters were as above but annealing and synthesis steps were shortened to 15 s. Annealing temperatures were optimized for each primer combination and were 65°C for CladAct.F1 with A14Act.R1, 66°C for CladAct.F1 with 4/97-2Act.R1 and for CladAct.F1 with 315WAct.R1, and 59°C for CladAct.F1 with A13Act.R1. Sets of appropriate positive and negative controls were included by using pure genomic DNA from appropriate strains of *Cladosporium* sp.

RESULTS

Morphological Characterization

To characterize the isolates from reed we first studied reference cultures (obtained from CBS) for the definition of typical characters recognizable by LTSEM in their native state. *C. oxysporum* CBS 125.80 (Fig. 1A), *C.*

tenuissimum CBS 674.82 (Fig. 1B), and *C. cladosporioides* CBS 401.80 (Fig. 1C) had smooth surfaces at lower magnifications. At higher magnification, *C. oxysporum* CBS 125.80 (Fig. 1G) and the other two smooth reference cultures exhibited a layer of rodlet fascicles on the whole conidial surface including the connections. Such structures corresponded to agglomerated hydrophobins (Wosten and de Vocht, 2000). Conidia of these strains showed considerable variation in branching patterns, size, and shape (not shown). These characters were therefore of limited value and not used for further differentiation. *C. herbarum* CBS 812.71 (Fig. 1D) exhibited digitate ornamentation, with rounded projections on the surface. *C. cladosporioides* CBS 169.54 (Fig. 1E) showed granulate ornamentations with rounded discrete projections. The different appearances of *C. cladosporioides* CBS 169.54 and CBS 401.80 observed by LTSEM provided first hints for problematic assignments of reference cultures.

When analyzing the isolates from reed by LTSEM three distinct types of conidia were found. Conidia of the first type, represented by isolates A14 (Fig. 2A) and 4/97-2 (Fig. 2B), were smooth, exhibiting rodlets at high magnifications identical to those of *C. oxysporum* CBS 125.80, *C. tenuissimum* CBS 674.82, and *C. cladosporioides* CBS 401.80. Other characters (conidium size, branching patterns, etc.) were highly variable. The second type, represented by isolate 315W (Fig. 2C), exhibited surface ornamentations identical to those of *C. herbarum* CBS 812.71. The third type, represented by isolate A13 (Fig. 2D), showed at higher magnifications irregular aculeate projections that were found neither in any of the reference cultures studied here nor in others (David, 1997). The ambiguities seen with some reference cultures prompted further molecular studies aimed to better characterize the isolates from reed.

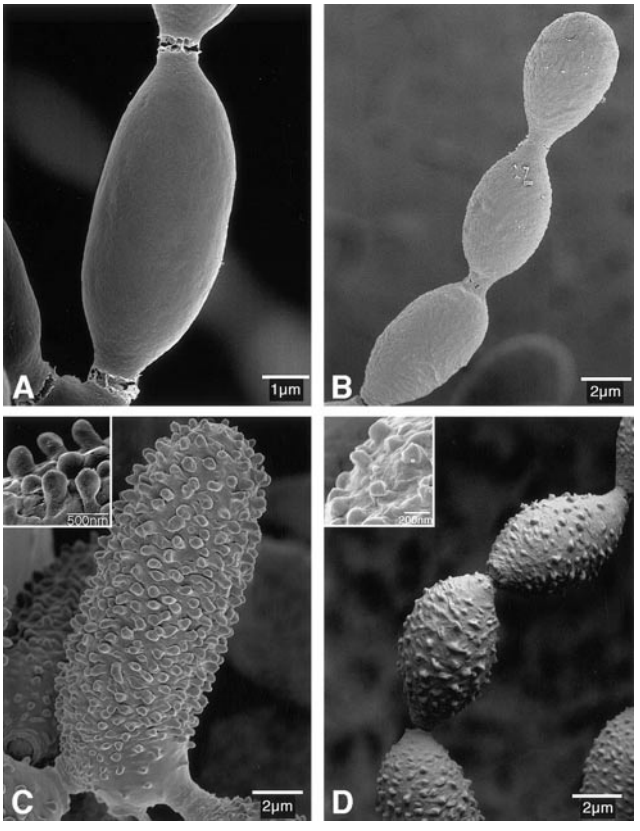

FIG. 2. LTSEM of native conidia from *Cladosporium* isolates recovered from *Phragmites australis.* (A) isolate A14; (B) isolate 4/97-2; (C) isolate 315W; (D) isolate A13. For details of isolates, see Table 1.

Genetic Diversity of Cladosporium Sp. from Reed

Pairwise comparisons of all sequences from our reed isolates revealed four different ITS sequence types, designated A–D (see Table 1). Overall, the sequences were quite similar, 94.2% being the lowest score with ITS type D versus type A or type B. Types A and B exhibited only one varying nucleotide separating the morphotype characterized as *C. oxysporum* (see Figs. 2A and 2B) into two subgroups. Type A was identical to both the ITS sequences from *C. oxysporum* CBS 125.80 and *C. cladosporioides* CBS 401.80. *C. tenuissimum* CBS 674.82 had only one exchanged nucleotide compared to ITS type A. Type B did not find a perfect match. The correlation of ITS type C with the *C. herbarum* morphotype was further validated by its identity to the ITS sequence from *C. herbarum* CBS 812.71. ITS type D corresponding to the *Cladosporium* sp. represented by isolate A13 matched neither any of our reference sequences nor those currently deposited in public databases. The second reference culture included in this study for *C. cladosporioides* (CBS 169.54) was different from *C. cladosporioides* CBS 401.80 by five nucleotides and did not match any sequence of the reed-associated Cladosporia.

To embed our new sequences within a broader phylogenetic context established in the literature, we assembled a phylogenetic tree comprising all ITS sequences for *Cladosporium* currently deposited in public databases, one sequence for ITS types A to D and all seven reference cultures sequenced in this study (Fig. 3). All entries displayed belong to plant-associated Cladosporia since medically relevant Cladosporia were recently shown to be only distantly related to the former (Masclaux *et al.*, 1995). One

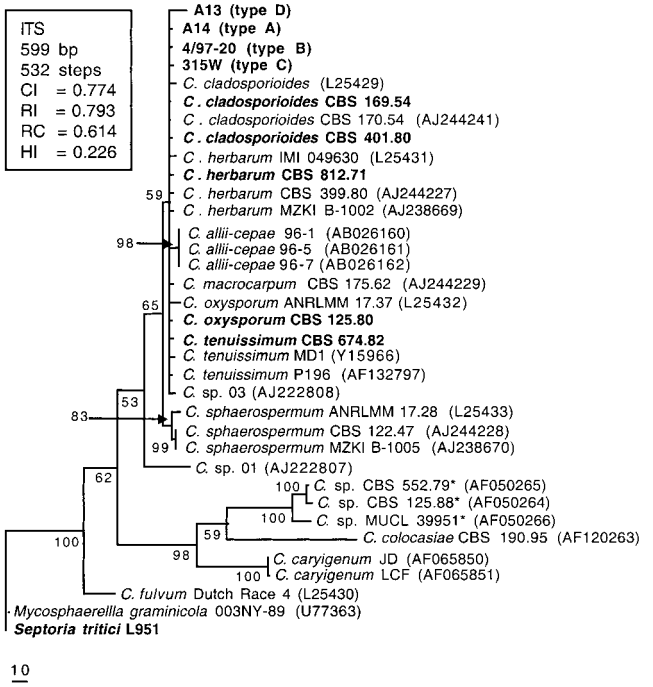

FIG. 3. Phylogram displaying the relationships between four different types (A–D) of ITS1–5.8S–ITS2 rDNA sequences from *Cladosporium* spp. isolated from reed and reference cultures. Sequences established during this study are in boldface. References, which were taken from EMBL and GenBank databases, are in plain type. Accession numbers are indicated in parentheses. The tree was generated by maximum-parsimony using 1000 bootstrap replicates in the program PAUP 4.0.d64. *CBS 552.79, CBS 125.88, and MUCL 39951 were reassigned as *Capronia* spp. (Untereiner and Naveau, 1999).

large unresolved clade (59% bootstrap support) comprised strains assigned to *C. cladosporioides, C. oxysporum, C. tenuissimum, C. herbarum,* and *C. macrocarpum.* Bootstrap-supported branches lead to *C. allii-cepae* (leaf blotch on onion and leek), *C. sphaerospermum, Cladosporium* spp. accessions AF050264–AF050266 (isolates from wood, reassigned as *Capronia* spp. (Untereiner and Naveau, 1999)), and *C. caryigenum* (scab on pecan).

To derive a more detailed molecular phylogeny for species within the unresolved part of the tree we also determined partial actin sequences for a subset of 23 isolates from reed and the seven reference cultures. The PCR primers FungAct.F1 and FungAct.R1 (see Table 3) were directed against conserved regions of currently known fungal actin genes to amplify fragments from codon 84 to codon 342. We detected an intron inserted at exactly the same position (after codon 299) in the actin PCR fragments from all Cladosporia analyzed, but also in the related *S. tritici.* The sequence of this intron was highly variable. After excising the introns and translating to peptide sequences, BLASTP searches revealed that the closest matches in current databases are the actins from *Botrytis cinerea, Acremonium chrysogenum,* and *Aspergillus nidulans.* These genes also have an intron at the very same position (data not shown). With the exception of *C. fulvum* and *S. tritici,* all peptide sequences determined in this study were identical since nucleotide variations generally corresponded to silent changes. The same subset of 30 strains was utilized to generate a phylogeny for the actin gene and, for comparison, for the ITS region. The lower diversity of the sequences used to generate this second ITS tree (Fig. 4A)—when compared to that shown in Fig. 3—generally increased the bootstrap support above 50%, now separating ITS types A–D (Fig. 4A). *C. oxysporum* CBS 125.80, *C. tenuissimum* CBS 674.82, and *C. cladosporioides* CBS 401.80 clustered with ITS type A and *C. herbarum* CBS 812.71 with ITS type C, whereas ITS types B and D and *C. cladosporioides* CBS 169.54 remained on separate branches. The corresponding actin tree (Fig. 4B) mirrored the separation of the ITS types A–D seen in Fig. 4A, but exhibited higher resolution leading to further differentiation in terminal branches. Here, ITS type B formed two sister clades but bootstrap support for the monophyly of type B was below 50% (data not shown).

The topologies of ITS and actin trees were confirmed to be highly concordant ($P = 0.99$) by a partition homogeneity test. Therefore, both datasets were combined and analyzed using the total evidence (Fig. 4C). The branching pattern of the combined tree was highly similar to that seen in the actin tree with the exception of branches comprising *C. cladosporioides* CBS 169.54 and *C. tenuissimum* CBS 674.82.

Physiological Diversity of Cladosporium Sp. from Reed

The above analysis revealed four putative species of *Cladosporium* that were all recovered from the same host species. Furthermore, we discovered a high genetic diversity at the population–species interface. This raised the question whether there were physiological differences at the species or infraspecific levels that might indicate specialization for the location or host habitat or host organ from where these isolates were initially retrieved. Therefore, we analyzed the substrate utilization patterns of 18 isolates from reed (see Table 1) on 95 different carbon sources implemented in BIOLOG SF-N microtiter plates. The resulting growth patterns (Table 4) were used to create a phylogenetic tree by parsimony analysis (Fig. 5).

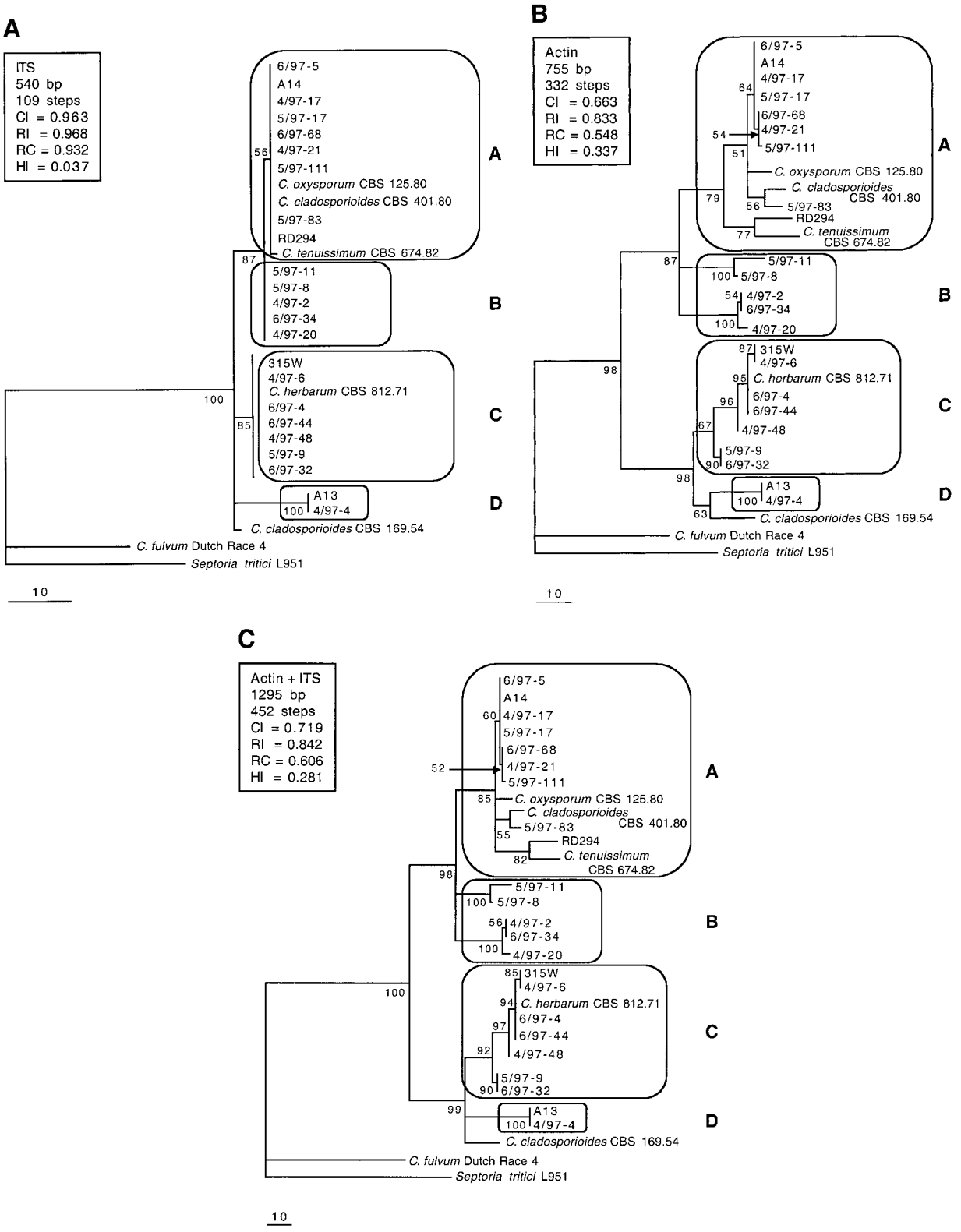

FIG. 4. Phylogram displaying the relationships between 23 Cladosporia from reed and seven additional reference cultures. (A) ITS-tree; (B) actin tree; (C) combined ITS–actin tree. The trees were generated by maximum-parsimony using 1000 bootstrap replicates with the program PAUP 4.0.d64. (A) ITS types A, C, and D form separate monophyletic clades with bootstrap values above 50%. ITS type B forms an unresolved cluster adjacent to type A. (B) and (C) show similar topologies with better bootstrap support for the monophyly of the types A, C, and D. In addition type B forms two sister clades to type A.

TABLE 4
Carbon Catabolite Spectra of Reed-Associated Cladosporia on BIOLOG SF-N Microtiter Plates

Isolate	Carbon sources 1 to 96 integrated in BIOLOG plates[a]																							
	1	10	20	30	40	50	60	70	80	90	96
315W	0	0	3	3	2	2	3	3	2	3	0	2	3	3	2	3	2	1	1	2	3	3	2	2	3	3	0	1	2	0	2	0	1	0	0	2	3	3	2	3	2	2	3	0	2	0	1	2	2	3	0	2	0	0	3	0	0	0	0	2	0	0	3	0	0
6/97-4	0	0	3	3	2	2	3	3	2	3	0	2	3	3	2	3	2	1	1	2	3	3	2	2	3	3	0	2	3	0	2	0	1	0	0	2	3	3	2	3	2	2	3	0	2	0	1	2	2	3	0	2	0	0	3	0	0	0	0	2	0	0	3	0	0
4/97-6	0	0	3	2	1	2	0	2	2	2	3	2	3	0	0	1	0	0	2	0	2	0	0	1	0	0	2	2	0	0	3	1	1	0	2	0	0	1	0	2	1	0	0	2	0	0	1	1	2	2	0	1	0	0	2	0	0	0	0	2	0	0	3	0	0
6/97-32	0	0	3	3	1	2	0	2	3	2	3	2	2	2	0	1	2	2	2	2	2	3	0	2	1	0	0	1	2	0	2	0	0	0	0	0	1	0	0	0	2	1	3	1	0	1	1	0	2	0	0	1	0	2	1	0	1	0	0	0	0	0	2	0	0
5/97-9	0	0	3	2	1	2	0	3	3	3	2	2	2	1	1	2	3	2	1	3	3	3	0	2	3	0	0	1	2	0	2	0	0	0	0	0	2	0	0	0	2	1	2	2	1	0	2	1	1	0	2	1	0	0	1	2	1	0	2	0	0	1	0	0	0
4/97-48	0	0	3	2	2	0	3	3	3	3	3	3	3	3	3	2	2	3	3	3	3	3	0	2	3	0	0	1	2	0	0	2	3	2	0	3	1	3	2	1	0	3	2	2	2	2	2	0	1	1	0	2	2	2	3	2	0	2	0	0	0	0	0	2	0	0	3
A14	0	0	3	2	3	3	0	3	3	3	3	3	3	3	3	3	3	3	3	3	3	3	0	2	0	3	3	3	2	0	3	3	3	2	3	0	1	2	0	0	2	2	0	2	0	1	2	1	3	1	0	1	0	2	2	2	0	3	2	2	3	2	2	0	0	0	2	0	0	3
RD294	0	0	3	3	3	1	3	3	3	3	3	3	3	3	3	3	3	3	3	3	3	3	0	2	3	2	2	3	0	2	2	3	0	2	2	2	0	0	0	2	2	1	0	1	3	2	3	2	0	3	0	3	2	2	3	3	2	2	2	3	2	2	0	3	0	2	0	0	3	3
5/97-111	0	0	3	2	3	0	3	3	3	3	3	3	3	3	3	3	3	3	3	3	3	3	0	2	3	0	3	3	2	0	3	3	3	2	3	1	1	2	0	0	2	1	0	2	1	2	2	0	0	0	2	2	1	0	2	2	1	3	3	0	2	2	1	2	0	2	0	0	3	2
4/97-17	0	0	3	2	3	0	3	2	3	3	3	3	3	3	3	3	3	3	3	3	3	3	0	2	3	0	3	3	2	0	3	3	3	2	3	0	1	2	0	0	2	1	0	2	1	2	2	0	0	0	2	2	3	3	2	2	1	2	2	0	3	0	0	0	1	2	0	0	3	3
4/97-2	0	0	3	3	3	0	2	3	3	3	3	3	3	3	3	3	3	3	3	3	3	3	0	2	2	0	2	0	2	0	1	0	0	0	2	2	0	0	1	2	3	1	0	2	3	2	2	1	2	2	3	2	0	3	2	1	2	2	0	2	0	0	0	0	0	2	0	0	3	2
5/97-11	0	0	3	3	3	0	3	3	3	3	3	3	3	3	3	3	3	3	3	3	3	3	0	2	3	0	3	0	3	0	3	3	3	2	3	2	1	2	0	0	2	3	0	3	0	0	0	0	1	0	0	2	3	3	1	0	3	3	1	2	3	1	0	3	0	0	0	0	2	3
5/97-17	0	0	3	3	3	0	2	2	3	2	3	0	3	3	3	3	3	3	3	3	3	3	0	2	3	0	2	2	0	2	0	3	3	2	3	2	2	1	0	2	2	0	0	0	2	1	3	0	2	0	2	2	1	3	0	2	0	0	0	0	2	0	0	0	2	0	0	0	2	0	0	1
6/97-68	0	0	3	3	2	2	0	2	2	3	2	3	3	3	3	3	3	3	3	3	3	3	0	2	3	0	2	2	0	3	0	3	3	2	3	2	2	1	0	2	2	0	0	0	2	1	3	0	2	0	2	2	1	3	0	2	0	0	0	0	2	0	0	0	2	0	0	0	2	0	0	1
6/97-2	0	0	3	2	2	3	3	3	3	3	3	3	3	3	3	3	3	3	3	3	3	3	0	2	3	0	3	0	3	0	3	3	3	2	3	2	2	1	0	2	2	0	0	0	2	1	3	0	2	0	2	2	1	3	0	2	0	0	0	0	2	0	0	0	2	0	0	0	2	0	0	1
6/97-5	0	0	3	2	3	3	3	3	3	3	3	3	3	3	3	3	3	3	3	3	3	3	0	2	3	0	3	0	3	0	3	3	3	2	3	2	2	1	0	2	2	0	0	0	2	1	3	0	2	0	2	2	1	3	0	2	0	0	0	0	2	0	0	0	2	0	0	0	2	0	0	1
4/97-4	0	0	3	2	2	3	3	0	3	3	3	3	3	3	3	2	1	3	3	3	2	1	1	2	0	0	2	2	0	2	1	1	0	0	2	2	2	3	1	0	1	0	3	2	2	3	3	3	0	2	2	3	2	3	3	2	0	2	0	0	0	0	0	2	0	0	3
A13	0	0	3	2	2	3	0	3	3	3	3	3	3	3	3	2	0	3	3	3	2	1	1	2	0	0	2	2	0	2	1	1	0	0	0	0	0	1	1	0	0	0	2	2	3	1	0	1	0	2	2	3	2	2	3	2	0	3	0	0	0	0	0	2	0	0	3

Note. Isolates were sorted according to the order obtained in the phylogeny shown in Fig. 5.

[a] Growth patterns were scored from 0 (no growth) to 3 (maximal growth) as detailed under Materials and Methods and recorded in numerical order from carbon source 1 to 96. For reference, negative (no carbon source, well 1) and positive controls (glucose, well 18) are underlined. Carbon sources that differentiated the major groups are indicated by boldface. These were from left to right: l-fucose, beta-methyl-d-glucoside, d-raffinose, sucrose, l-Ala, l-Asn, l-Asp, l-Glu, hydroxy-l-Pro, l-Leu, l-Pro, l-Thr, and phenylethylamine.

Analyses with the Wagner method with equal weights gave identical results (data not shown). Strains with ITS type C (*C. herbarum*) formed a monophyletic clade, whereas strains belonging to ITS types A and B (*C. oxysporum*) remained unseparated. The two isolates for ITS group D (A13 and 4/97-4) that were distinguished by morphology and molecular analysis from the other groups were also differentiated by the BIOLOG analysis. Groupings at the terminal branches did not indicate correlation with location, habitat, or organ where the fungi were originally isolated. In addition, the topology of the *C. herbarum* clade seen in the BIOLOG tree was not identical to that seen in the actin tree (see Fig. 4B). Most of the differences underlying the tree shown in Fig. 5 are caused by poorer growth of *C. herbarum* on certain carbon sources compared with other groups. This was the case with several amino acids including l-Ala, l-Asn, l-Asp, l-Glu, l-Leu, l-Pro, and l-Thr, but also with l-fucose, d-raffinose, and sucrose (see Table 4).

Nested PCR Assay for Differentiation of Cladosporium Sp. in Reed DNA

The highly variable intron sequence discovered in the actin genes from *Cladosporium* spp. allowed the development of a nested PCR strategy for tracking closely related fungi in DNA preparations isolated from *P. australis.* Reactions with fungal genomic DNA were used to control the specificity of the conditions for PCRs with reed DNA as template. Figure 6A shows that all templates yielded bands (440 bp) after the first PCR step with primers targeting sequences conserved within the actin genes from all Cladosporia analyzed. We were able to differentiate between the four targets by using nested primers in the second PCR step that took advantage of the divergent sequences in the intron. As shown in Fig. 6A only DNA of the targeted strain produced the respective band (310–330 bp) but not DNA of the three other strains.

We used total DNA isolated from roots, stems, and leaves of eight reed plants harvested in August and from roots and shoots of eight plants harvested in April to compare the distribution of the different Cladosporia on reed at peak biomass and at the beginning of the growing season, respectively. All DNA preparations were initially controlled for general amplificability by a PCR assay directed against the ITS region of *P. australis* (Figs. 6B and 6C) and then used for the four nested PCRs. This approach allowed patterns of cocolonization to be deduced, i.e., how many different Cladosporia were present on the

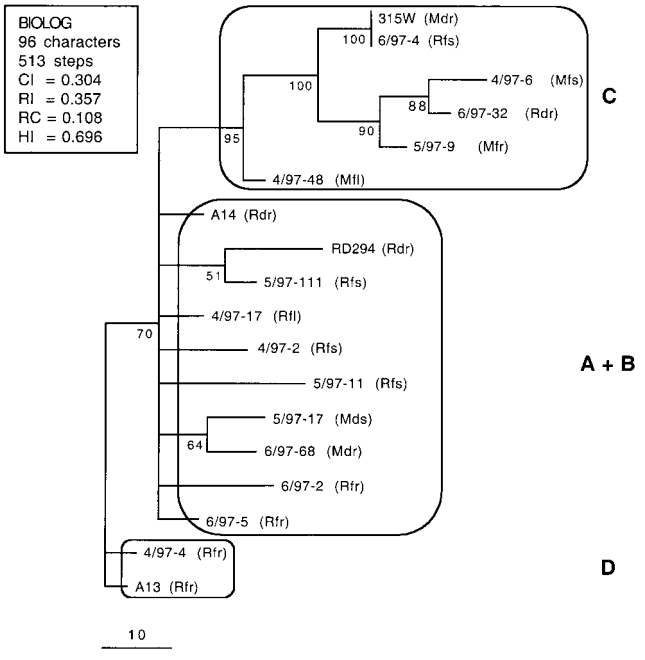

FIG. 5. Phylogram displaying the relationships between 18 Cladosporia from reed as derived from carbon utilization patterns of BIOLOG microtiter plates. Letters in parentheses designate the sampling histories of the respective strains as shown in Table 1, i.e., R/M, location: Reichenau/Mainau; f/d, position in reed belt: flooded/dry; r/s/l, host organ: root/stem/leaf. The tree was generated by maximum-parsimony using a matrix that weighted the growth differences according to four classes (see Table 4). Only branches with bootstrap values above 50% are presented.

respective organs of each reed plant. In 10 of the 24 August samples we could not detect any of the Cladosporia under investigation, whereas 6 samples had just one detectable type (Fig. 6C). In 4 samples we observed two different fungi and in 2 samples three and four different fungi, respectively. There was no apparent exclusion of any group by any other. In April samples these fungi were much rarer than in August samples with the exception of *Cladosporium* sp. type A13 which might have the ability to colonize the host earlier than others.

DISCUSSION

Species belonging to the genus *Cladosporium* are ascribed a variety of life styles ranging from saprotrophic, through epiphytic or endophytic, to pathogenic or even mycoparasitic (Ellis, 1971; David, 1997; Moricca *et al.*, 1999). We have recovered a collection of Cladosporia from common reed that could theoretically fall into any of these types. The sampling covered two locations at Lake Constance with two habitat types each, one being permanent and the other just rarely flooded. Furthermore, sampling differentiated between host organ, i.e., leaf, stem, and root. Isolates falling into the genus *Cladosporium* appeared to be generally recoverable from all organs and all sites. Here, we first differentiate these *Cladosporium* isolates by DNA sequence analysis and conidium surface ultrastructure as visualized by LTSEM and then address the ecology of these fungi.

Cladosporium is an anamorph genus. Classically, species within the genus were defined based on the morphological species concept but examination of the literature indicated repeated problems with assignments (De Vries, 1967; Ellis, 1971, 1976; Dugan and Roberts, 1994; David, 1997; Harrington *et al.*, 2000). In an earlier, smaller-scaled study, ITS data were used to establish a molecular phylogeny (Curtis *et al.*, 1994). Here, we combine both approaches to advance the current taxonomy of *Cladosporium*.

LTSEM revealed three distinct kinds of conidia among the reed-associated *Cladosporium* isolates. One was identified as *C. oxysporum*, one was typical for *C. herbarum*, and for the last we did not find a matching reference. The first showed smooth conidial surfaces; the other two showed distinctly ornamented surfaces. To investigate the development of the latter we observed younger stages (not shown) in addition to those differentiated conidia depicted here. Young conidia were initially smooth and the extrusions appeared to eventually break from the inside through the hydrophobin layer. We did not observe the rodlet layer on mature extrusions under the conditions employed.

A phylogeny constructed from all currently available ITS sequences did not allow unambiguous linkage of our strains to established species, probably because of too little sequence variation within certain groupings of plant-associated Cladosporia. We found *C. fulvum* basal to the other species of that genus. Most *Septoria* are now being placed in *Stagonospora*, which forms a monophyletic genus in the Leptosphaeriaceae (Cunfer and Ueng, 1999). In contrast, *M. graminicola* (anamorph: *S. tritici*) appeared to be only distantly related to *Stagonospora*, which questioned the grouping of *C. fulvum* and *M. graminicola* to their respective genera (Cunfer and Ueng, 1999).

A second ITS phylogeny created from a subset of sequences originating from 23 reed isolates and seven reference cultures resolved the same three clusters seen with LTSEM but additionally separated one of those—the *C.*

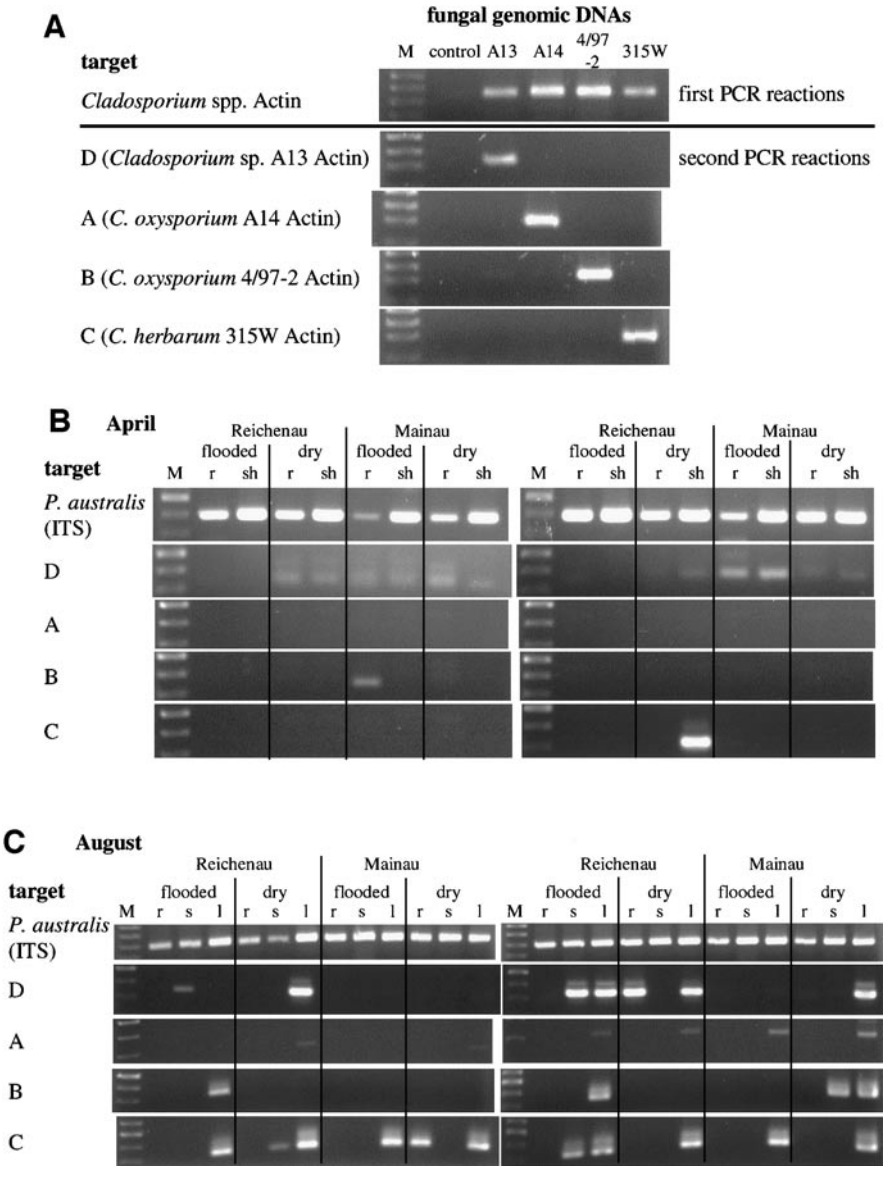

FIG. 6. Nested PCR detection of *Cladosporium* spp. in reed samples. (A) Specificity control with pure fungal genomic DNA as template. Lanes M, 100-bp size marker; control, no DNA included; A13 to 315W, fungal genomic DNA from the respective strains (details in Table 1). Target, specifies the amplified DNA, i.e., *Cladosporium* spp., first step of nested PCR amplified actin gene fragments from all Cladosporia; A–D, second steps of nested PCR used as templates aliquots from the first step and amplified only actin gene subfragments from *Cladosporium* types A to D as represented by the indicated strains. (B) Nested PCR on reed DNA isolated from eight plants harvested in April from four sites at Lake Constance. Target, *P. australis* (ITS), amplification control of template DNA with host-directed ITS primers. Other targets as in (A). Lanes M, 100-bp size marker; remaining lanes, PCR on template DNA isolated from two organs of reed (r, root; sh, shoot) grown at the four indicated sampling sites. (C) Nested PCR on reed DNA isolated from eight plants harvested in August from four sites at Lake Constance. Targets, see (B). Lanes M, 100-bp size marker; remaining lanes, PCR on template DNA isolated from three organs of reed (r, root; s, stem; l, leaf) grown at the four indicated sampling sites.

oxysporum type—into two subclades that differed only by one nucleotide. Interestingly, all strains with smooth conidial surfaces clustered together, as did all isolates with rough-walled conidia, thus reflecting a division among plant-associated Cladosporia. The rough-walled group was further distinguishable by the type of wall ornamentation. This was only possible with LTSEM at high resolution but again produced the same separations seen in the molecu-

lar phylogeny. High-resolution LTSEM combined with molecular phylogeny also indicated inconsistencies with reference cultures that might have arisen from limitations of conventional light microscopy and the variability of asexual morphological structures often seen within this genus. David (1997) found that conidial surface ornamentations at the light microscopic level are not reliable enough to consistently distinguish species within *Cladosporium;* however, at least in the subset of species analyzed here, we found congruency of high-resolution SEM with molecular data. Whether this will hold true when analyzing representatives from all described species of this genus will have to await future studies. These studies may also elucidate whether the smooth conidial type is primitive and the ornamented type a derived character in this group of fungi. This is indicated since both *C. fulvum* (Fig. 1F) and *M. graminicola* (Duncan and Howard, 2000) have smooth conidia like those in our groups A and B, whereas groups C and D and *C. cladosporioides* CBS 169.54 form a well-supported clade of fungi exhibiting distinctly ornamented conidia (see Fig. 4).

The value of using DNA sequences from intron-containing genes to study fungal evolution at the species/population interface has been shown in several studies using different types of genes (Geiser *et al.,* 1998; Carbone and Kohn, 1999; O'Donnell *et al.,* 2000). Alpha actin is an evolutionarily conserved component of the cytoskeleton and is encoded in filamentous ascomycetes by a single-copy gene (Carbone and Kohn, 1999; Tarkka *et al.,* 2000). A molecular phylogeny established from partial actin gene sequences produced the same overall topology as the ITS tree but differentiated the isolates at a higher resolution. Based on the morphological species concept, groups A and B belong to the same species. In the context of a phylogenetic species concept, groups A and B appear as separate species. Actin data not only divided A from B but also showed further separations within the A, B, and C groups. Phylogenies of additional protein-encoding genes could determine how many cryptic species are present within these groups. For the moment, a conservative judgement would be that we have recovered at least four different species from reed.

The indistinguishable morphology and the close molecular similarity of the three CBS strains in ITS group A carrying different species designations (see Fig. 4) emphasizes the need to taxonomically reevaluate the whole genus on a broader scale. A multilocus genealogy supported by LTSEM studies involving more genes and more isolates originating from various geographical regions should be used to redefine species borders within *Cladosporium.*

TABLE 5

Kishino–Hasegawa Test of Constrained and Unconstrained Trees from Combined ITS and Actin Datasets

Tree[a]	Tree length[b]	SD of difference[c]	t[d]	P[e]
MPT (unconstrained)	206	Best	Best	Best
Constrained for location	273 (+67)	11.02849	6.0752	<0.0001
Constrained for habitat	230 (+24)	7.1897	3.3412	0.0009
Constrained for organ	266 (+60)	10.2615	5.8470	<0.0001

[a] The combined ITS/actin dataset was identical to that used in Fig. 4C except for the reference strains. Rearrangements to generate constrained trees concerned branches within each of the groups A–D shown in Fig. 4C.

[b] Numbers in parentheses show differences between the most parsimonious tree (MPT) and the respective constrained tree.

[c] SD of log likelihood.

[d] Pairwise t test.

[e] Probability of getting a more extreme t value under the null hypothesis of no difference between the compared trees by using the two-tailed test. All results are significant at $P < 0.05$.

LTSEM and molecular taxonomy based on ITS and actin sequences conclusively show that the reed-associated Cladosporia are not homogenous but fall into at least four species. We used three approaches, one statistical, one physiological, and one molecular, to investigate evidence for ecological specialization. First, we enforced topological constraints on the branches of a combined ITS/actin tree to simulate putative specialization according to sampling location, host habitat, and host organ. The trees comprised the same reed strains as those depicted in Fig. 4C but none of the reference cultures (data not shown). Rearrangements were in such a way that all isolates belonging to one ITS type remained in one cluster but terminal branches were exchanged accordingly. All of the constrained trees were significantly worse than the unconstrained most parsimonious tree as analyzed by the Kishino–Hasegawa likelihood test ($P > 0.05$) (Table 5). Therefore, the hypothesis that the phylogenetic separation seen within reed-associated Cladosporia is in concordance with host location, host habitat, and host organ can be rejected.

Second, we derived carbon catabolite fingerprints resulting from BIOLOG microtiter assays to investigate putative correlations with taxonomy at any level and/or with sampling details. Plant-associated fungi are obviously exposed to different carbon sources depending on the colonized host tissue. In addition, the spectrum of exudates from a given organ might vary with respect to habitat conditions. Fungi living in different habitats could therefore exhibit distinct carbon catabolite spectra—even

within a species—as has been shown in a study with *Fusarium compactum* and related species (Talbot *et al.,* 1996). The phylogeny derived from carbon catabolite spectra of reed-associated Cladosporia followed the morphological separations, i.e., again showed the C and D groups and the combined A and B groups. Whether the observed segregation of isolates is ecologically relevant is currently unclear since all species appeared to be present on all plant organs when both sampling records and PCR results are taken into account. The BIOLOG data also did not indicate physiologically specialized subpopulations within these species that would correlate with location, host habitat, or host organ. On the other hand, on a given organ different fungal species/populations might occupy different ecological microniches, for instance, the surface, the subcuticular space, or the apoplast.

Third, we used a nested PCR assay to distinguish the four different types of *Cladosporium* in DNA isolated from reeds growing at the same sites from where these fungi were initially recovered. By including samples harvested in April, we took into account that *P. australis* is a perennial grass that overwinters to emerge with young shoots every spring. These grow rapidly during the summer, reaching heights of 4 m at our locations. Three of the four Cladosporia were either missing or detected just once among 16 April samples analyzed. These belonged to ITS types A (*C. oxysporum*), B (*Cladosporium* sp.), and C (*C. herbarum*). *C. oxysporum* and *C. herbarum* are considered cosmopolitan (David, 1997) and were recovered from many different plant hosts, sometimes after surface sterilization procedures as we did (Petrini *et al.,* 1992; Pelaez *et al.,* 1998). On the other hand, the fourth type, i.e., *Cladosporium* sp. (ITS type D), was detected in several plants that had just emerged about 2 weeks prior. This might hint at a capacity to colonize reeds earlier than the others or at a systemic nature of this particular fungus. When analyzing plants harvested in August, at peak biomass, we found that these fungi are more common and colonized all host organs without clear preference for any sampling site, except for *C. oxysporum* (ITS type A). This fungus was detected by PCR only in leaf DNA, whereas sampling data also indicated its presence in other organs (Table 1), a difference that could have been caused by the fewer number of plants analyzed in the PCR assay.

Our results show that reed sympatrically hosts several species of *Cladosporium* that do not appear to be specialized for host organ or host habitat. If they would grow exactly at the same space and time, they might compete with each other. The analysis of cocolonization patterns did not reveal obvious antagonistic effects between the four types at the macroscopic level studied. A related study analyzed putative specialization of two sympatric species within the *Botrytis cinerea* species complex, which colonizes many plant species (Giraud *et al.,* 1997). It was suggested that the more pathogenic species was a local adaptation in the Champagne region of France and that the more saprophytic species was a migrant. In addition to grapes, both were also detected later on several other host plants. Significant differences in their distribution correlated with host species but not with host organs or locations (Giraud *et al.,* 1999). The genus *Cladosporium* comprises ubiquitous species (e.g., *C. herbarum*) and host-specific species (e.g., *C. colocasiae*) (Ellis, 1971, 1976). Our data show that some of our isolates are very similar or even identical to reference cultures with respect to ITS and actin sequences, e.g., 6/97-4 and 6/97-44 to *C. herbarum* CBS 812.71 (see Fig. 4). Since the CBS strains originate from other host plants (see Table 2) it has to be concluded that the respective reed isolates do not appear to be specialized for this host. Other isolates are more distantly related to the reference cultures analyzed here, especially those included in the ITS groups B and D (see Fig. 4). It might be possible that these exhibit host preferences which could be analyzed by the nested PCR protocol developed during this work.

In summary, we have shown that fungi recovered from reed and initially assigned to the genus *Cladosporium* actually comprise at least four different species: *C. herbarum, C. oxysporum,* and two different *Cladosporium* spp. This finding highlights how diverse the reed-associated mycoflora might finally be, since *Cladosporium* was just 1 from at least 16 fungal genera found to be closely associated with *P. australis* (Wirsel *et al.,* 2001). None of several lines of investigation confirmed putative specialization of the different Cladosporia for host habitats or host organs. On the other hand, distinct temporal patterns of colonization or subtle specialization at the tissue level may characterize the different species. A combination of molecular and advanced visualization techniques such as *in situ* PCR might be able to increase the level of resolution necessary to address some of these questions.

ACKNOWLEDGMENTS

This project was financially supported by the SFB 454 from the Deutsche Forschungsgemeinschaft. We gratefully acknowledge John C. David (CABI, U.K.) for the characterization of strains and Walter Gams and Sybren de Hoog for helpful comments on the manuscript. We thank

Michael Ernst, Ralf T. Voegele, Christine Struck, and Matthias Hahn for discussions.

REFERENCES

Carbone, I., and Kohn, L. M. 1999. A method for designing primer sets for speciation studies in filamentous ascomycetes. *Mycologia* **91:** 553–556.

Cunfer, B. M., and Ueng, P. P. 1999. Taxonomy and identification of *Septoria* and *Stagonospora* species of small grain cereals. *Annu. Rev. Phytopathol.* **37:** 267–284.

Curtis, M. D., Gore, J., and Oliver, R. P. 1994. The phylogeny of the tomato leaf mould fungus *Cladosporium fulvum* syn. *Fulvia fulva* by analysis of rDNA sequences. *Curr. Genet.* **25:** 318–322.

David, J. C. 1997. *A Contribution to the Systematics of* Cladosporium: *Revision of the Fungi Previously Referred to* Heterosporium. CAB Int., Oxon, U.K.

De Vries, G. A. 1967. *Contribution to the Knowledge of the Genus* Cladosporium *Link ex. Fr.* Cramer, Lehre, Germany.

Dobranic, J. K., and Zak, J. C. 1999. A microtiter plate procedure for evaluating fungal functional diversity. *Mycologia* **91:** 756–765.

Dugan, F. M., and Roberts, R. G. 1994. Morphological and reproductive aspects of *Cladosporium macrocarpum* and *C. herbarum* from bing cherry fruits. *Mycotaxon* **52:** 513–522.

Duncan, K. E., and Howard, R. J. 2000. Cytological analysis of wheat infection by the leaf blotch pathogen *Mycosphaerella graminicola. Mycol. Res.* **104:** 1074–1082.

Ellis, M. B. 1971. *Dematiaceous Hyphomycetes.* CAB Int., Kew, UK.

Ellis, M. B. 1976. *More Dematiaceous Hyphomycetes.* CAB Int., Kew, UK.

Gardes, M., and Bruns, T. D. 1993. ITS primers with enhanced specificity for Basidiomycetes—Application to the identification of mycorrhizae and rusts. *Mol. Ecol.* **2:** 113–118.

Geiser, D. M., Pitt, J. I., and Taylor, J. W. 1998. Cryptic speciation and recombination in the aflatoxin-producing fungus *Aspergillus flavus. Proc. Natl. Acad. Sci. USA* **95:** 388–393.

Giraud, T., Fortini, D., Levis, C., Lamarque, P., Leroux, P., LoBuglio, K. F., and Brygoo, Y. 1999. Two sibling species of the *Botrytis cinerea* complex, *transposa* and *vacuma*, are found in sympatry on numerous host plants. *Phytopathology* **89:** 967–973.

Giraud, T., Fortini, D., Levis, C., Leroux, P., and Brygoo, Y. 1997. RFLP markers show genetic recombination in *Botryotinia fuckeliana* (*Botrytis cinerea*) and transposable elements reveal two sympatric species. *Mol. Biol. Evol.* **14:** 1177–1185.

Harrington, T. C., Steimel, J., Workneh, F., and Yang, X. B. 2000. Molecular identification of fungi associated with vascular discoloration of soybean in the North Central United States. *Plant Disease* **84:** 83–89.

Masclaux, F., Guého, E., De Hoog, G. S., and Christen, R. 1995. Phylogenetic relationships of human-pathogenic *Cladosporium* (*Xylohypha*) species inferred from partial LS rRNA sequences. *J. Med. Vet. Mycol.* **33:** 327–338.

Moricca, S., Ragazzi, A., and Mitchelson, K. R. 1999. Molecular and conventional detection and identification of *Cladosporium tenuissimum* on two-needle pine rust aeciospores. *Can. J. Bot.* **77:** 339–347.

O'Donnell, K., Kistler, H. C., Tacke, B. K., and Casper, H. H. 2000. Gene genealogies reveal global phylogeographic structure and reproductive isolation among lineages of *Fusarium graminearum*, the fungus causing wheat scab. *Proc. Natl. Acad. Sci. USA* **97:** 7905–7910.

Pelaez, F., Collado, J., Arenal, F., Basilio, A., Cabello, A., Matas, M. T. D., Garcia, J. B., DelVal, A. G., Gonzalez, V., Gorrochategui, J., Hernandez, P., Martin, I., Platas, G., and Vicente, F. 1998. Endophytic fungi from plants living on gypsum soils as a source of secondary metabolites with antimicrobial activity. *Mycol. Res.* **102:** 755–761.

Petrini, O., Sieber, T. N., Toti, L., and Viret, O. 1992. Ecology, metabolite production, and substrate utilization in endophytic fungi. *Nat. Toxins* **1:** 185–196.

Swofford, D. L. 2000. Phylogenetic Analysis Using Parsimony (* and Other Methods), Sinauer, Sunderland, MA.

Talbot, N. J., Vincent, P., and Wildman, H. G. 1996. The influence of genotype and environment on the physiological and metabolic diversity of *Fusarium compactum. Fungal Genet. Biol.* **20:** 254–267.

Tarkka, M. T., Vasara, R., Gorfer, M., and Raudaskoski, M. 2000. Molecular characterization of actin genes from homobasidiomycetes: Two different actin genes from *Schizophyllum commune* and *Suillus bovinus. Gene* **251:** 27–35.

Untereiner, W. A., and Naveau, F. A. 1999. Molecular systematics of the Herpotrichiellaceae with an assessment of the phylogenetic positions of *Exophiala dermatitidis* and *Phialophora americana. Mycologia* **91:** 67–83.

White, T. J., Bruns, T., Lee, S., and Taylor, J. 1990. Amplification and direct sequencing of fungal ribosomal RNA genes for phylogenetics. In *PCR Protocols: A Guide to Methods and Applications* (M. A. Innis, D. H. Gelfand, J. J. Sninsky, and T. J. White, Eds.), pp. 315–322, Academic Press, New York.

Wirsel, S. G. R., Leibinger, W., Ernst, M., and Mendgen, K. 2001. Genetic diversity of fungi closely associated with common reed. *New Phytol.* **149:** 589–598.

Wosten, H. A., and de Vocht, M. L. 2000. Hydrophobins, the fungal coat unravelled. *Biochim. Biophys. Acta* **1469:** 79–86.